ACS OMEGA

Open Access

http://pubs.acs.org/journal/acsodf

Article

Rutin Promotes Wound Healing by Inhibiting Oxidative Stress and Inflammation in Metformin-Controlled Diabetes in Rats

Published as part of ACS Omega virtual special issue "Phytochemistry".

Manal Naseeb, Eram Albajri, Arwa Almasaudi, Turki Alamri, Hatoon A. Niyazi, Soad Aljaouni, Abdulrahman B. O. Mohamed, Hanouf A. Niyazi, Ahmed S. Ali, Soad Shaker Ali, Saber H. Saber, Huda Ahmed Abuaraki, Shafiul Haque, and Steve Harakeh*

Cite This: *ACS Omega* 2024, 9, 32394−32406

Read Online

ACCESS | Metrics & More | Article Recommendations

ABSTRACT: Diabetes mellitus (DM) is a metabolic disorder with a notable increase in global incidence in recent years. Individuals diagnosed with diabetes are at an elevated risk of morbidity and mortality compared with the general population. For several years, the potential of phytochemicals as anti-inflammatory agents to improve the healing of diabetic wounds has been under investigation. Rutin, a flavonoid, is a particularly promising candidate for use in wound healing. Our study aims to investigate the potential impact of a topical application of rutin nanoformulation on wound healing in streptozotocin (STZ)-induced hyperglycemic rats controlled with metformin, with a focus on its anti-inflammatory and antioxidant properties. Rats are randomized into 3 groups. GI: diabetic control group; wound untreated. GII: diabetes and rutin-NP-treated wound. GIII: diabetic + β-sitosterol-treated wound. The findings suggest that topical application of rutin-NPs has the potential to enhance the wound-healing process by attenuating oxidative stress, as evidenced by restoring GSH, CAT, and SOD antioxidants, and decreasing MDA production mediated by Nrf2 activation. Also, inflammation is suppressed, as indicated by the decreased CRP, IL-1β, IL-6, and TNF-α levels. Molecular docking data confirm the biological data of rutin, where rutin is docked into the catalytic site of the X-ray crystallographic structures of CRP, Keap-1, IL-1β, IL-6, and TNF-α via grid-based ligand docking. The binding affinity and binding energy of ligand−protein interactions demonstrate the affinity and binding to the specifically selected proteins.

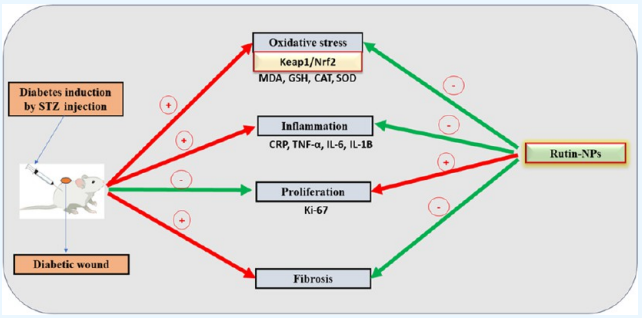

1. INTRODUCTION

Diabetes mellitus (DM) is a metabolic disorder that has led to a notable increase in global incidence in recent years. Individuals diagnosed with diabetes are at an elevated risk of morbidity and mortality compared to the general population. The International Diabetes Federation projected that in 2015, there were 415 million individuals aged 20 to 79 living with diabetes, with estimates suggesting this number may reach 642 million by 2040.[1] Furthermore, diabetes-related health expenditure and fatalities reached a staggering $673 billion and 5 million, respectively.[1]

Wound healing in diabetic patients is characterized by a prolonged inflammatory phase with increased levels of cytokines, such as tumor necrosis factor-α (TNF-α), interleukin (IL)-1β, and IL-6.[2] This overproduction of cytokines leads to increased tissue damage and delayed diabetic wound healing. Also, prolonged hyperglycemia increases reactive oxygen species (ROS) production and oxidative injury.[3,4] Therefore, the primary reason for a longer healing time in diabetic wound patients is prolonged inflammation, and attenuation of inflammation and oxidative stress is essential to expedite the healing of diabetic wounds.

For several years, the potential of phytochemicals as anti-inflammatory agents for improving the healing of diabetic wounds has been under investigation.[5] Flavonoids, a class of natural pigments found in fruits and vegetables, have been shown to have beneficial effects on the onset of diabetes. Rutin, a flavonoid found in buckwheat, is a particularly promising candidate for wound healing.[6] Multiple studies have demonstrated that rutin possesses antioxidative, anti-inflammatory, neuroprotective, nephroprotective, and hepatoprotective prop-

Received: July 31, 2023
Revised: February 9, 2024
Accepted: February 14, 2024
Published: March 13, 2024

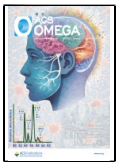

erties.[7−10] In medical practice, a variety of medications have been extensively utilized to promote wound healing. Chemically derived drugs are expensive and have adverse risks.[11] It is still necessary to research new compounds that can aid in the healing of wounds. The use of natural remedies for treating wounds has rapidly expanded recently.[12−14] Although several phytochemicals have asserted that they have the ability to heal wounds, the majority of these assertions lack robust scientific evidence.[12] Moreover, compared to conventional treatment methods, nanomaterial-based wound healing has a lot of potential for treating and preventing wound infections.[15] Our study aimed to investigate the potential impact of rutin-NPs on wound healing in streptozotocin (STZ)-induced hyperglycemic rats, with particular attention to their anti-inflammatory and antioxidant properties.

2. MATERIALS AND METHODS

2.1. Animals. In this investigation, 30 adult male Wistar rats were used. They were obtained from the Laboratory Animal Unit, King Fahd Medical Research Center, King Abdulaziz University, Jeddah, Kingdom of Saudi Arabia. The animals age was 7−8 weeks old, and their average body weight was 210−230 g. They were housed in groups of 10 animals each and were maintained in a controlled environment at room temperature of 20 ± 2 °C, relative humidity of 40−65%, and a 12 h day and night cycle. After wound induction, each rat was placed in a separate cage. The rats were fed conventional rodent chow. The rats had free access to food and water throughout the day. Before the start of the experiment, animals were kept in their cages for 7 days for acclimatization, and animal procedures were performed according to the animal unit at King Fahd Medical Research at the King Abdulaziz University ethical standards, which are based on the Declaration of Helsinki as an internationally agreed justificatory framework for handling animals used for research. The CEMGR ethical committee approved the animal experimental procedure (IRP: 27-CEGMR-Bioteth-2021).

2.2. Induction of Diabetes in Rats. A single intraperitoneal (i.p.) injection of 45 mg/kg STZ diluted in 0.01 M citrate buffer, pH 4.5, was administered to the diabetic group of rats to induce type II diabetes. After 72 h of STZ injection, blood from the tail vein was tested for fasting glucose levels using Accu-Chek Advantage strips (Roche, Germany). Animals with blood glucose levels of over 250 mg/dL were considered diabetic. Metformin was used to control diabetes.

2.3. Synthesis of Rutin-Nanoparticles (Rutin-NPs). As mentioned in the literature, the rutin-NP employed in this research was formulated using a double emulsion method that involved encapsulating rutin within PLGA and PVA natural polymers, along with the addition of Pluronic 127, a nonanionic surfactant, as previously documented.[16,17]

2.4. Characterization of Rutin-NPs. The zeta potential and size of rutin-NPs while dispersing in water were determined using dynamic light scattering (DLS) and electrophoretic light scattering (ELS) techniques, as outlined in our earlier publications on using nanoparticles of ellagic or pomegranate.[18,19]

2.5. Assessment of Encapsulation Efficiency (EE) and Loading Ratio (LR). The encapsulation efficiency (EE) of rutin-NPs was assessed by calculating the proportion of rutin contained within the nanoparticles relative to the initial quantity introduced, as outlined in eq 1

$$\mathrm{EE} = \frac{\text{encapsulated rutin quantity} \times 100}{\text{initial rutin quantity}} \quad (1)$$

The loading ratio (LR) was determined by calculating the proportion of encapsulated rutin in relation to the total weight of the resulting nanoparticle generated, as depicted in eq 2

$$\mathrm{LR} = \frac{\text{encapsulated rutin quantity} \times 100}{\text{total weight of preparation}} \quad (2)$$

2.6. Induction of Wounds in Diabetic Rats. After 4 weeks of induction of diabetes, a full-thickness wound was created as follows. The rats were anesthetized using a cocktail mixture of ketamine and xylazine (50 mg/kg and 5 mg/kg, respectively). Carprofen was used as an analgesic agent three times daily at a dose of 5 mg/kg BW, SC for 3 days after wound induction.[20]

Hair was removed from the rat's dorsal surface with an electric shaving machine without any damage to the stratum corneum and sterilized with 75% ethyl alcohol. A marker was used to mark the wound site in an area of 1 cm × 1 cm. Sharp scalpels were used to create an excisional wound on the dorsal backs of the animals after anesthetization. The rats were randomized into 3 groups (n = 10 per group). GI: diabetic control group; wound untreated. GII: diabetes + rutin-NP-treated wound. GIII: diabetic + β-sitosterol (standard)-treated wound. Metformin was used to control diabetes at a dose of 300 mg/kg.[21]

2.7. Topical Treatment Design. A topical preparation of both rutin-NPs and β-sitosterol (standard) on diabetic wounds of glycemic diabetic rats was controlled by metformin and used as a topical supplement to full-thickness wounds in diabetic rats. For 21 days, the wound was coated with a constant amount (1 mL) of the prior formulation after cleaning with sterile saline. The nanoparticles were prepared by dissolving the powder in a sterile double-distilled water solution and stirring into commercially bought Vaseline to give a final concentration of 1.59 mg/g, which was used for daily application.

2.8. Biochemical Assays. Serum TG, total cholesterol (TC), and high-density lipoprotein (HDL) levels were assayed using kits from Spinreact (Spain). Low-density lipoprotein (LDL) was calculated according to the following equation: (total cholesterol−HDL cholesterol−triglycerides)/5.

2.9. Histopathological Examinations. The procedure for histological preparation was as described by Bancroft and Stevens.[22] Skin tissues were thinly sliced to a thickness of 3−4 μm, fixed in 10% neutral-buffered formalin (10% NBF), dehydrated in ethanol, cleaned in xylene, and then embedded in paraffin.[23] To analyze the general tissue structure, the paraffin blocks were sectioned with a microtome at 5 μm thickness and stained with hematoxylin and eosin and Masson's trichrome stain. A light microscope was used to view the H&E and Masson trichrome-stained sections.

2.10. Assessment of Skin Oxidative Injury. Malondialdehyde (MDA) and reduced glutathione (GSH) contents and the activities of superoxide dismutase (SOD) and catalase (CAT) were determined in the supernatant of the homogenized skin. The GSH content was determined using the method described by Ellman.[23] By using this technique, the amount of yellow color that the nitromercaptobenzoic acid exhibits is directly connected to the GSH concentration. Using spectrophotometry, the absorbance was determined at 412 nm. The methods described by Uchiyama and Mihara were used to quantify the amount of MDA. These methods were based on the finding that the combination of TBA and MDA produces a pink hue that can be measured at 535 and 520 nm.[24] The amount of

https://doi.org/10.1021/acsomega.3c05595
ACS Omega 2024, 9, 32394−32406

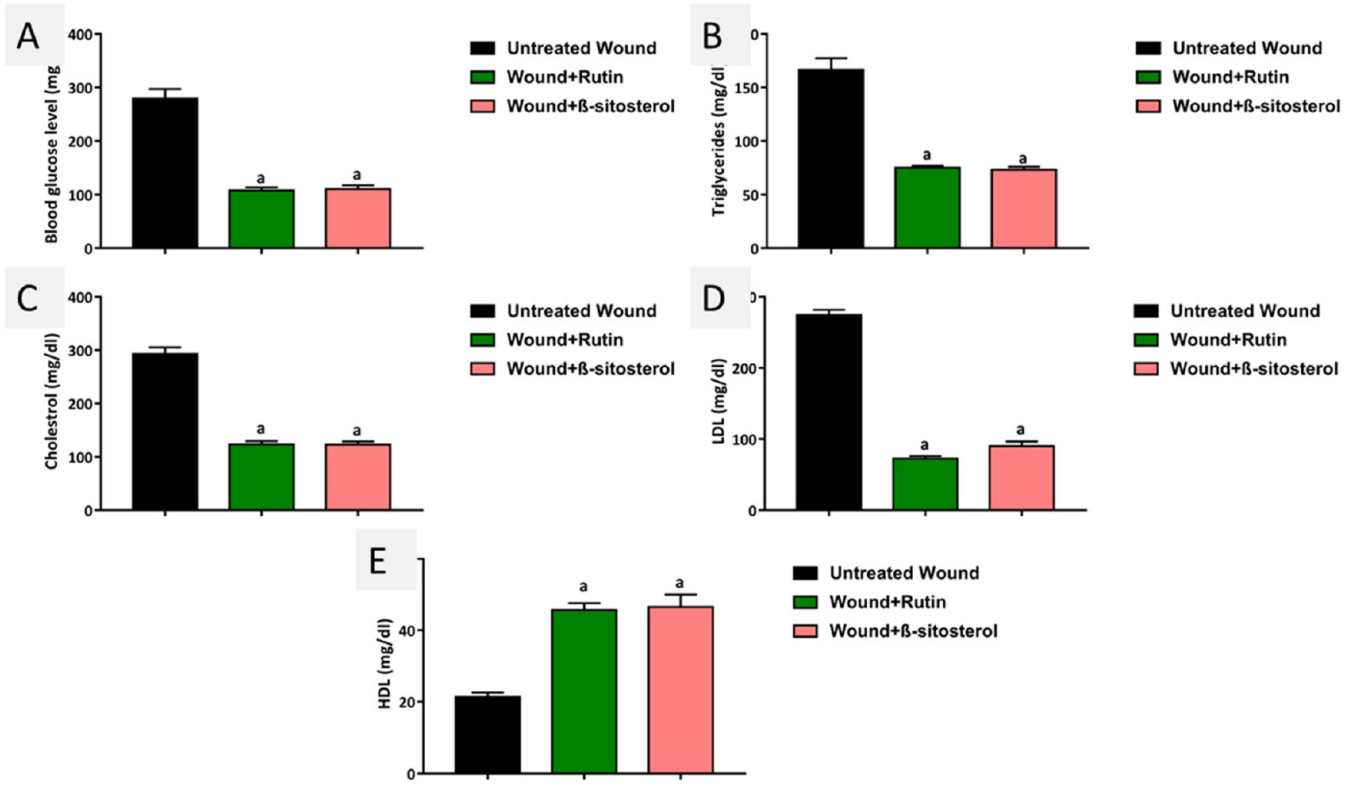

Figure 1. Effect of topical rutin-NP wound treatment in metformin-treated diabetic rats on hyperglycemia and hyperlipidemia markers. Rutin-NP topical application with metformin attenuated hyperglycemia and hyperlipidemia in STZ-induced diabetes in rats. Topical application with rutin-NPs with metformin significantly decreased blood glucose (A), TG (B), cholesterol (C), and LDL (D) levels and increased HDL (E) levels. [a] Significantly different from diabetic control rats. [b] Significantly different from the rutin group, $P < 0.05$.

CAT present in the rat tissues was determined by measuring the absorbance at 240 nm, which decreased as a result of CAT breaking down to H_2O_2.[25] The SOD enzymatic activity was measured using Marklund and Marklund's methodology. The ability of SOD to prevent pyrogallol autoxidation is necessary for their activity. The SOD activity of the tested samples and its inhibition are closely related. For 3 min, the absorbance at 420 nm was measured at 1 min intervals.[26]

2.11. Assessment of Circulating CRP and Proinflammatory Cytokines, Including TNF-α, IL-1β, and IL-6. According to the guidelines, ELISA kits from ELabscience were used to measure the concentrations of CRP, TNF-α, IL-1β, and IL-6. All kit instructions and processes were followed exactly, as prescribed by the manufacturer. Antibodies specific for rat CRP, TNF-α, IL-1β, and IL-6 were precoated on a microplate. Any rat CRP, TNF-α, IL-1β, and IL-6 that may be present were bound by the immobilized antibody prior to the standard, control, and sample-filled wells were pipetted with a substrate solution. The application of the stop solution caused the blue product of the enzyme to turn yellow. At 450 nm, the color's intensity was measured.[27]

2.12. Immunohistochemistry. The deparaffinized sections were subjected to rehydration, two microwave heating cycles for antigen retrieval, treatment with 3% H_2O_2, and incubation with 5% goat serum albumin. Following overnight incubation at 4 °C with primary anti-Nrf2 antibody, dilution 1:100 (supplied by Biospes, Chongqing, China), primary anti-Keap-1 antibody, dilution 1:100 (supplied by Biospes, Chongqing, China), and primary anti-K_i-67 antibody, dilution 1:100 (supplied by Biospes, Chongqing, China), the sections were treated for 1 h with HRP-conjugated goat antirabbit secondary antibody before visualization using a DAB kit. The slides were examined under a microscope following hematoxylin counterstaining.

2.13. Molecular Docking Analysis. Molecular docking was performed to predict the fit between rutin and the target proteins. The crystal structures of CRP, Keap-1, IL-1β, Il-6, and TNF-α were downloaded from the Protein Data Bank with PDB IDs 1B09, 4L7B, 9ILB, 1ALU, and 2AZ5, respectively.[28−32] The amino acid residues in the binding sites were considered for grid box adjustment. The three-dimensional structure of the ligand was retrieved from PubChem (CID_5280805) database in sdf format and converted into pdb format using Open Babel software.[33] All inhibitors and water molecules were removed from the downloaded structures. AutoDock vina was used for molecular docking studies of rutin with the target receptors.[34] The analysis and visualization of the ligand−protein interactions were performed by Biovia Discovery Studio visualizer software.[35] Based on the ligand docking results, the pose with the lowest binding energy was chosen as the best pose.

2.14. Statistical Analysis. The data were statistically analyzed and are presented as the mean ± standard error (SEM). Comparisons between the control and diabetic untreated groups were performed using a one-way analysis of variance (ANOVA) followed by Tukey's test. A P value < 0.05 was considered statistically significant.

3. RESULTS

3.1. Effect of Topical Application of Rutin-NPs on Hyperglycemia and Hyperlipidemia in STZ-Controlled Diabetes in Rats. As depicted in Figure 1, our findings indicate that the STZ group exhibited elevated glucose levels (Figure 1A) in comparison to the control group, as well as higher levels of TG

https://doi.org/10.1021/acsomega.3c05595
ACS Omega 2024, 9, 32394−32406

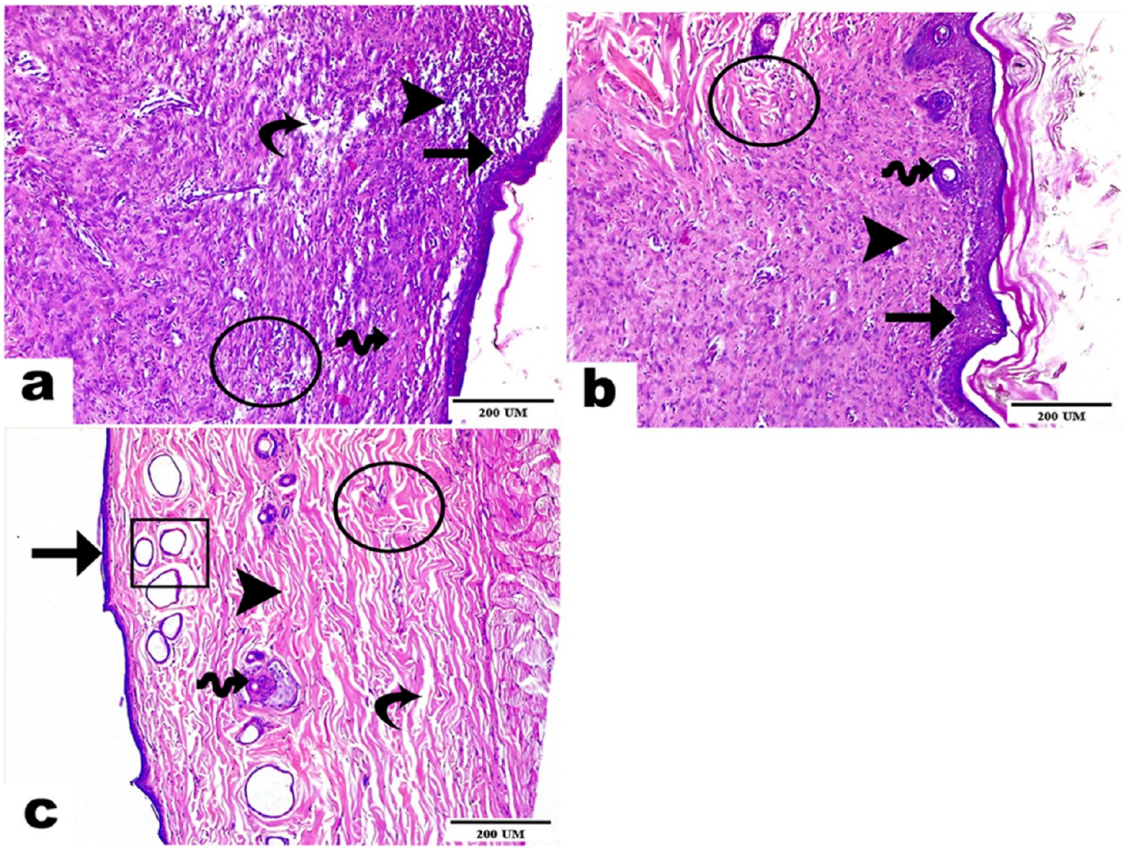

Figure 2. Topical applications of rutin-NPs attenuated skin histopathological findings in STZ-induced diabetic rats. Photomicrographs represented the effect of rutin-NPs on the histopathological changes in skin tissues at 21 days among the studied groups (hematoxylin & eosin stain, magnification power = ×100, and scale bar = 200 μm). (a) The skin section of the diabetic control group exposed to the epidermis with a developed detached scab above the wound surface (arrow). Besides, the subepidermal layer showed disorganized fibrous tissue and highly accumulated inflammatory cells (arrowhead). The dermis layer is marked by interstitial edema leading to dispersion between the fibrous connective tissue (curvy arrow) and intense interstitial infiltration of inflammatory cells (circle). (b) The skin section of rutin-NP-treated rats displayed an epidermis with a newly formed thick scab above the wound surface (arrow), few migrating epidermal cells (wave arrow), dermis with a large amount of fibrous connective tissue (arrowhead), and a moderate amount of inflammatory cell infiltration (circle). (c) The skin section of the β-sitosterol (standard)-treated group showed epidermis with a thin layer of newly formed epidermal layer (arrow) with a noticeable number of migrating epidermal cells (rectangle) besides noticeable progress in skin gland development (wave arrow). The dermis layer demonstrated well-organized fibrous connective tissue (arrowhead) and partial areas with interstitial edema (curvy arrow), besides a rare number of inflammatory cell infiltrations (circle).

(Figure 1B), cholesterol (Figure 1C), and LDL (Figure 1D), and a huge decline in HDL (Figure 1E). Conversely, treatment with metformin with topical application of rutin-NPs as well as β-sitosterol effectively mitigated these effects by reducing glucose levels and decreasing TG, LDL, and cholesterol levels as well as elevating HDL levels compared to the diabetic control group.

3.2. Rutin-NPs Attenuated Skin Histopathological Findings in STZ-Induced Diabetic Rats. Skin sections of the diabetic control group exposed the epidermis with a developed detached scab above the wound surface. Besides, the subepidermal layer contained disorganized fibrous tissue and highly accumulated inflammatory cells. The dermis layer is marked by interstitial edema, which leads to dispersion between the fibrous connective tissue and intense interstitial infiltration of inflammatory cells. Interestingly, the skin sections of rutin-NP-treated rats displayed an epidermis with a newly formed thick scab above the wound surface, a few migrating epidermal cells, a dermis with a large amount of fibrous connective tissue, and a moderate amount of inflammatory cell infiltration. The skin sections of the β-sitosterol (standard)-treated group showed the epidermis with a thin layer of a newly formed epidermal layer with a noticeable number of migrating epidermal cells besides noticeable progress in skin gland development. The dermis layer showed well-organized fibrous connective tissue and partial areas with interstitial edema, besides a rare number of inflammatory cell infiltrations (Figure 2).

3.3. Rutin-NPs Attenuated Skin Oxidative Injury in STZ-Induced Diabetic Rats. As demonstrated in Figure 3, our results showed that the lipid peroxidation MDA (Figure 3A) was increased, while the skin antioxidants GSH (Figure 3B), CAT (Figure 3C), and SOD (Figure 3D) levels were depleted in diabetic control rats. Conversely, the topical preparation of rutin-NPs successfully restored skin GSH, CAT, and SOD antioxidants and decreased skin MDA production, thus promoting wound healing. Furthermore, the results of the immunohistochemical analysis indicated that the STZ group displayed upregulation of Keap-1 (Figure 4) and lower expression levels of Nrf2 (Figure 5). In contrast, the application of rutin-NPs was found to counteract this effect and down-regulate Keap-1 while it upregulated Nrf2 levels (Figure 4).

3.4. Rutin-NPs Attenuated Inflammation in STZ-Induced Diabetic Rats. The present study demonstrates

https://doi.org/10.1021/acsomega.3c05595
ACS Omega 2024, 9, 32394−32406

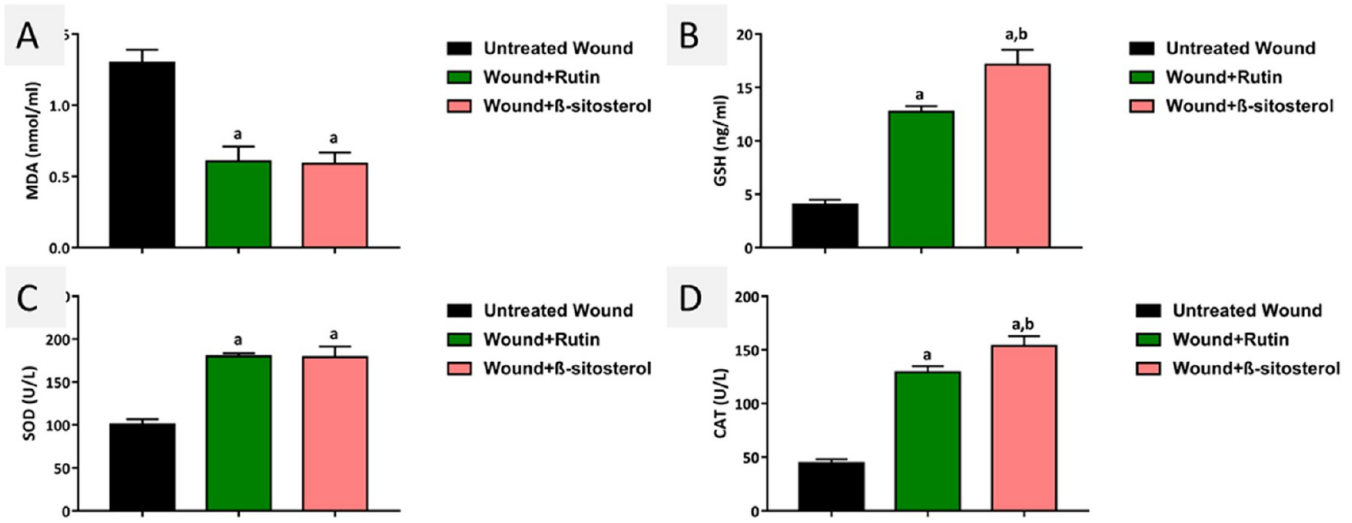

Figure 3. Effect of topical rutin-NP wound treatment in metformin-treated diabetic rats on skin oxidative stress biomarkers. Rutin-NP topical preparation attenuated oxidative stress in STZ-induced diabetes in rats. Rutin-NP topical preparation decreased lipid peroxidation MDA (A) and increased antioxidants GSH (B), SOD (C), and CAT (D). [a] Significantly different from diabetic control rats. [b] Significantly different from the rutin-NP group, $P < 0.05$.

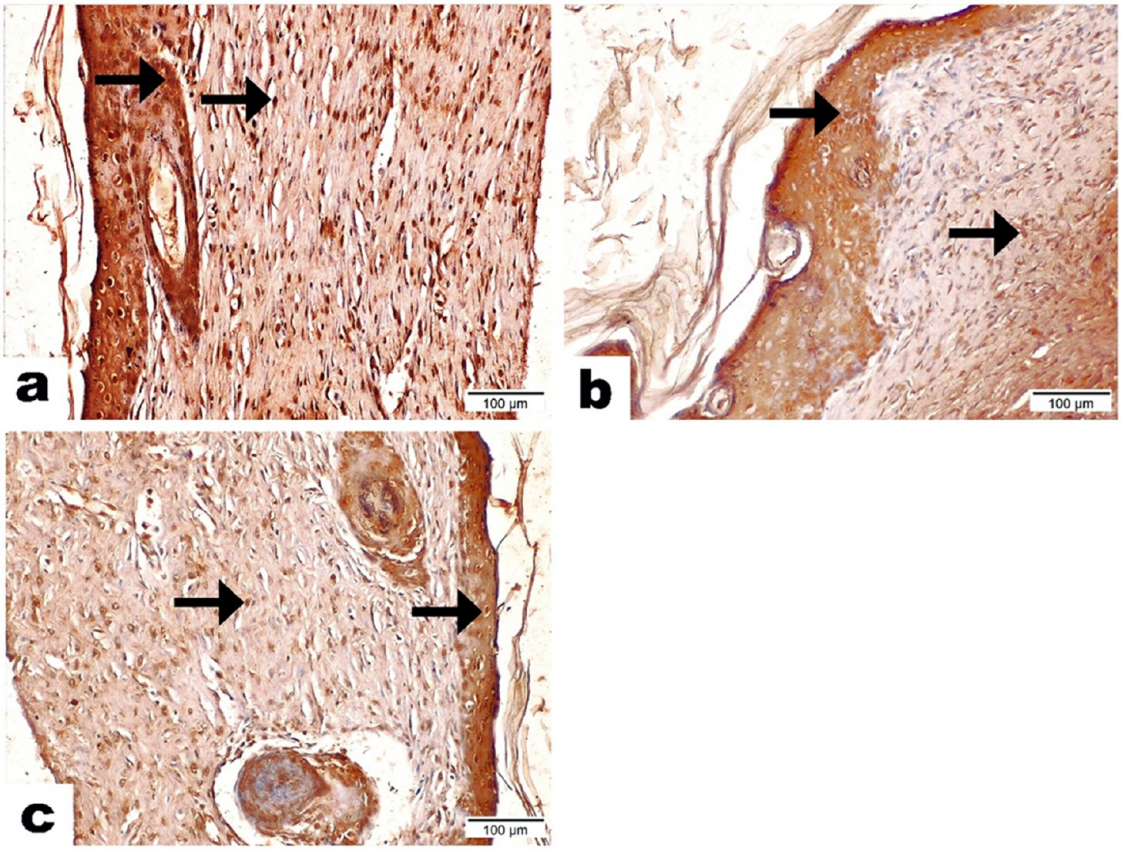

Figure 4. Effect of topical rutin-NP wound treatment in metformin-treated diabetic rats on Nrf2 expression profile. Rutin-NP topical preparation upregulates Nrf2 in STZ-induced diabetes in rats. Photomicrographs emphasized the reactivity of Nrf2 antibody along RT drug-treated groups in skin tissues at 21 days (Nrf2 antibody, magnification power = ×200, and scale bars = 100 μm): (a) skin section of the diabetic control group showed moderate Nrf2 expression lengthwise epidermal (arrow) and dermal layers (arrowhead). (b) Skin section of the rutin-treated group highlighted high Nrf2 expression along the epidermal (arrow) and dermal layers (arrowhead). (c) Skin section of β-sitosterol (standard) demonstrated Nrf2 antibody with intense responsiveness within the epidermal (arrow) besides dermal layers (arrowhead). [a] Significantly different from diabetic control rats. [b] Significantly different from the rutin-NP group, $P < 0.05$.

that the STZ-treated group exhibited elevated levels of inflammatory markers, such as CRP (Figure 6A) and proinflammatory cytokines, including TNF-α (Figure 6B), IL-1β (Figure 6C), and IL-6 (Figure 6D). Interestingly, topical

https://doi.org/10.1021/acsomega.3c05595
ACS Omega 2024, 9, 32394−32406

Table 1. Best Binding Energy Values (kcal/mol) and Binding Features of the Best-Docked Pose of the Ligand−Receptor Complex

protein	binding energies (kcal/mol)	binding features
Keap-1	−10.4	Ser363, Gly364, Leu365, Ser383, Asn414, Arg415, Ile416, Gly509, Leu557
CRP	−7.9	Ser44, Tyr49, Trp67, Val86, Thr90, Ala92, Val94, val111, Arg116
TNF-α	−8.7	Leu57, Tyr59, Gly121, Tyr151
IL-1β	−8.2	Ala1, Pro2, Ser5, Ser43, Lys63, Glu64, Tyr68, Lys88, Pro91, Ser153
IL-6	−6.6	Arg30, Leu33, Ser37, Gln175, Arg179, Arg182

treatment with rutin-NPs effectively counteracted this increase and significantly reduced the levels of these inflammatory mediators (Figure 6).

3.5. In Silico Evidence. A docking analysis was performed to investigate the molecular mechanisms by which rutin produces its effects and confirm the biological results. In this respect, rutin was docked into the catalytic site of the X-ray crystallographic structures of CRP, Keap-1, IL-1β, Il-6, and TNF-α via grid-based ligand docking. The binding affinity and binding scores of ligand−protein interactions are listed in Table 1.

The docking energy of binding of rutin with Keap-1 was −10.4 kcal/mol. The aromatic rings of rutin enable hydrophobic interactions with the hydrophobic residues of Keap-1. Rutin forms seven hydrogen bond interactions with Ser363, Gly364, Leu365, Ser383, Asn414, Ile416, and Leu557 at distances of 2.75, 2.72, 2.0, 2.32, 2.71, 2.96, and 2.61 Å respectively. Moreover, it forms π−alkyl and C−H interactions with Arg415 and Gly509 (Figure 7).

The catalytic domain of CRP covers around 47 amino acids and is considered critical for therapeutic and diagnostic purposes. The molecular docking of rutin with CRP showed a binding affinity of −7.9 kcal/mol and interactions with Ser44, Tyr49, Trp67, Val86, Thr90, Ala92, Val94, val111, and Arg116, which support the stable interaction of the rutin with this protein. These amino acid residues play critical roles in the anti-inflammatory response associated with CRP (Figure 8). Thus, the interaction of rutin with these residues is considered significant in clinical studies. TNF-α is an inflammatory cytokine produced during acute inflammation and is important to resist many infectious diseases. Molecular docking indicated that rutin exhibits an excellent binding energy of −8.7 kcal/mol and has a better binding affinity to the key residues of TNF-α. It forms two hydrogen bonds with Gly121 (2.37 Å) and Tyr151 (2.23 and 3.08 Å) that stabilize the ligand−protein complex. Furthermore, the aromatic ring forms one π−alkyl bond with Leu57 and two π−π bonds with the Tyr59 residue (Figure 9). Additionally, docking studies revealed that rutin has an excellent docking score of −8.2 kcal/mol with IL-1β. Rutin forms five hydrogen

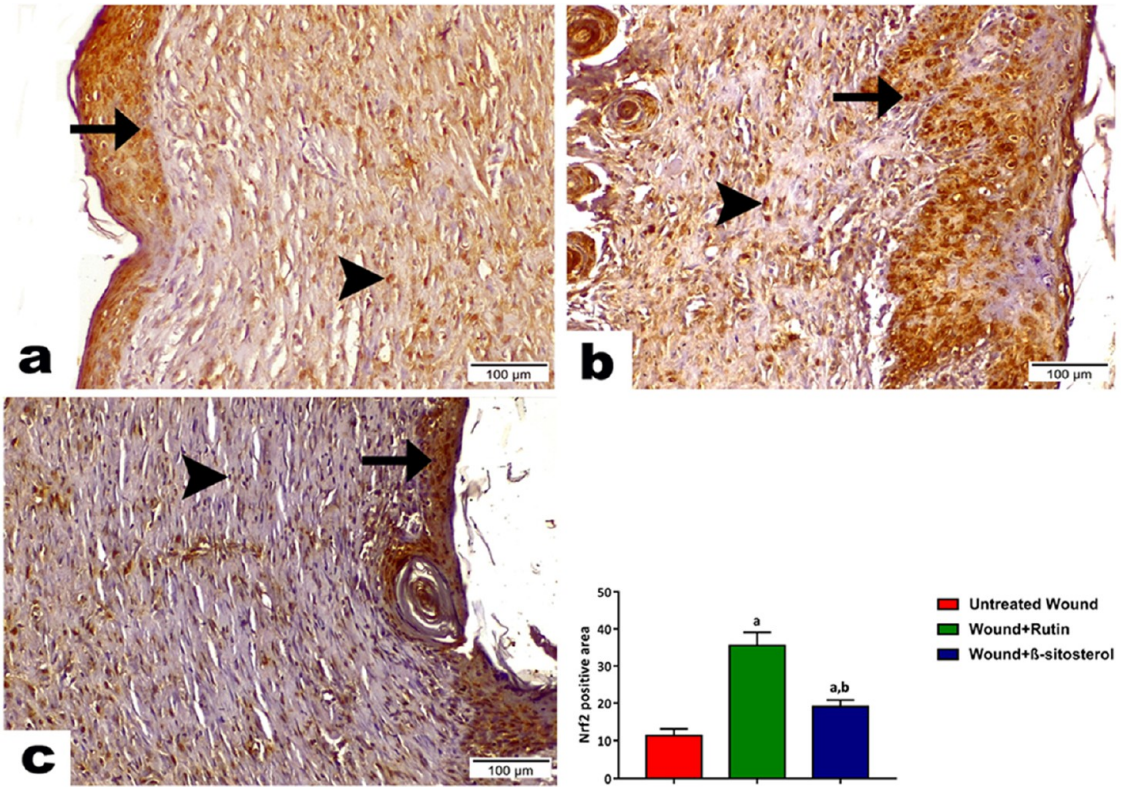

Figure 5. Topical preparation of rutin-NP downregulated Keap-1 in STZ-induced diabetic rats. Photomicrographs displayed the immunohistochemical reaction of Keap-1 antibody in skin tissues at 21 days among experimental groups stained with Keap-1 antibody (magnification power = 200×, scale bar = 100 μm): (a) The skin section from the untreated control group showed strong expression of Keap-1 antibody (+++) with cytoplasmic and nuclear reactivity along the epidermis and dermis layers (arrows). (b) The skin section from the rutin-NP-treated group exhibited moderate expression of Keap-1 antibody (++) with cytoplasmic and nuclear reactivity of the epidermis and dermis layers (arrows), with a significant difference from the negative control group. (c) The skin section from the β-sitosterol (standard)-treated group indicated low expression of Keap-1 antibody (+) with cytoplasmic and nuclear reactivity along the epidermis and dermis layers (arrows) with a significant difference from the untreated group and rutin-NP group.

https://doi.org/10.1021/acsomega.3c05595
ACS Omega 2024, 9, 32394−32406

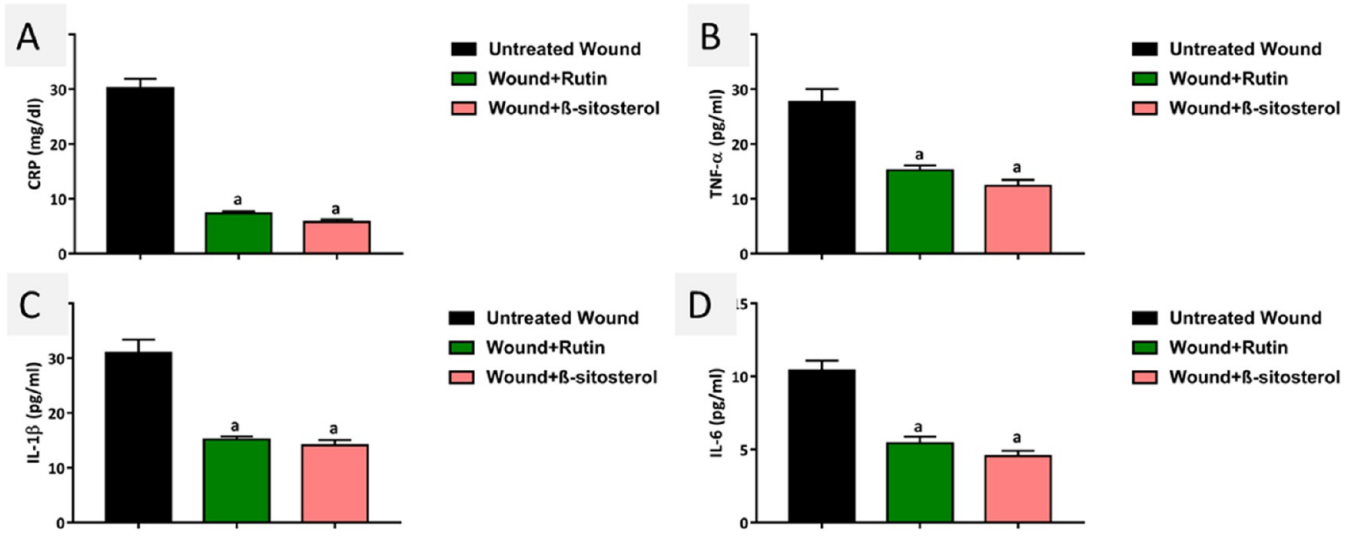

Figure 6. Effect of topical rutin-NP wound treatment in metformin-treated diabetic rats on skin inflammation parameters. Rutin-NP topical preparation attenuated inflammation in STZ-induced diabetes in rats. Our findings indicate that rutin-NP topical preparation decreased the levels of CRP (A) and circulating proinflammatory cytokines TNF-α (B), IL-1β (C), and IL-6 (D). [a] Significantly different from diabetic control rats. [b] Significantly different from the rutin group, $P < 0.05$.

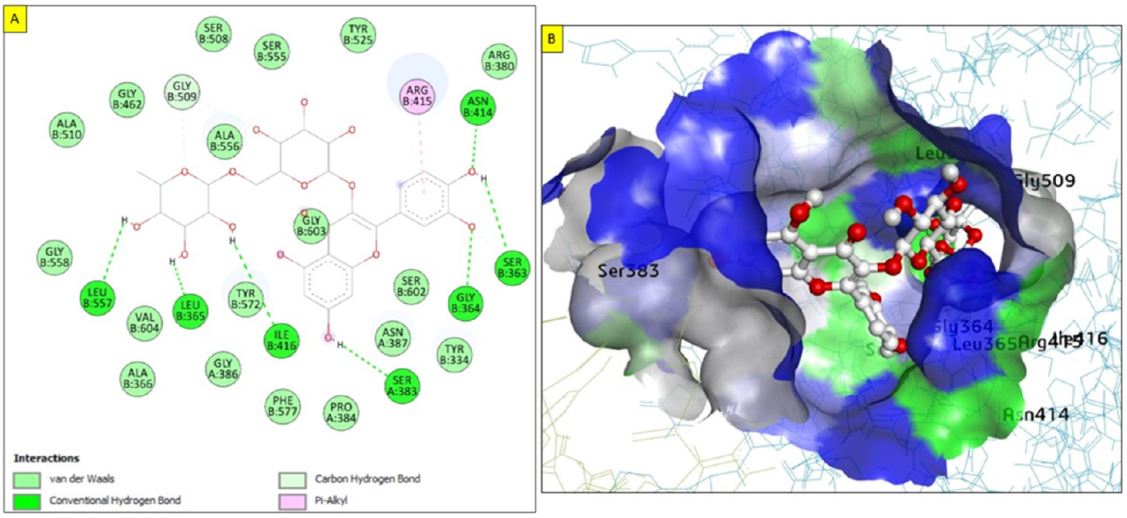

Figure 7. Molecular docking of rutin with Keap-1: (A) two-dimensional (2D) rutin−Keap-1 interaction, and (B) three-dimensional (3D) view of rutin in the active site of Keap-1.

bonds with Ser5 (3.06 Å), Ser43 (1.88 and 2.35 Å), Tyr68 (2.46 Å), Pro91 (2.71 Å), and Ser153 (2.06 and 2.49 Å). Also, it forms three π−alkyl bonds with Ala1, Pro2, and Lys63 in addition to π−anion and π−cation bonds with Glu64 and Lys88, respectively (Figure 10). In addition to the previous proteins, rutin fits well into the active site of IL-6 with a binding energy of −6.6 kcal/mol. Rutin forms several hydrogen bonds with the surrounding residues in the binding pocket of IL-6. These residues are Arg30 (2.34 Å), Leu33 (2.46 Å), Gln175 (2.16 Å), Arg179 (2.54 Å), and Arg182 (2.02, 2.70, and 2.90 Å). Moreover, it forms π−alkyl bonds with Leu33 and C−H bonds with Ser37 at a distance of 3.58 Å (Figure 11). All these findings suggest a modulatory effect, which may be considered as the main mechanism of action of rutin.

3.6. Topical Application of Rutin-NPs Upregulates K_i-67 in STZ-Induced Diabetic Rats. The skin section from the untreated control group showed low expression of the K_i-67 antibody with cytoplasmic and nuclear reactivity all along the epidermis and dermis layers. The skin section from the rutin-NP-treated group showed moderate expression of the K_i-67 antibody with cytoplasmic and nuclear reactivity of the epidermis and dermis layers, with a significant difference from the negative control group. The skin section from the β-sitosterol (standard) group showed the highest expression of the K_i-67 antibody with cytoplasmic and nuclear reactivity along the epidermis and dermis layers, with a significant difference from the untreated control group and rutin-NP group (Figure 12).

3.7. Effect of Topical Preparation of Rutin-NPs on Skin Fibrosis of Skin Stained with Masson's Trichrome Stain in STZ-Induced Diabetic Rats. The skin section from the untreated control group showed a loosely packed and irregular arrangement of collagen fibers along the dermis layer. The skin sections from the application of rutin-NP and β-sitosterol (standard) group showed the regenerated collagen bundles with the regular arrangement and extensive distribution homing the dermal layer (Figure 13).

https://doi.org/10.1021/acsomega.3c05595
ACS Omega 2024, 9, 32394−32406

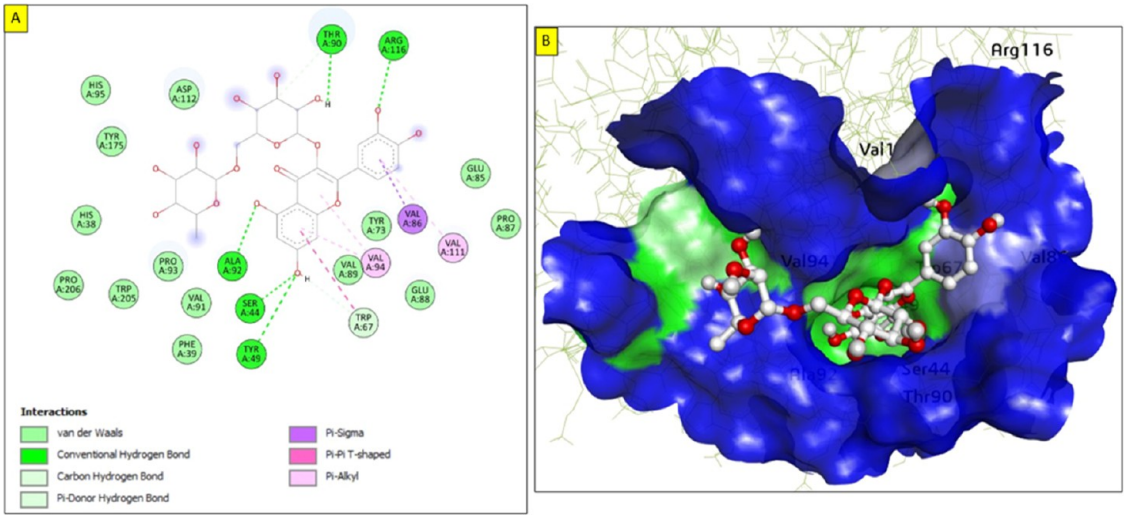

Figure 8. Molecular docking of rutin with CRP: (A) 2D interaction of rutin with CRP, and (B) surface view of the best-docked pose at the binding site of the protein.

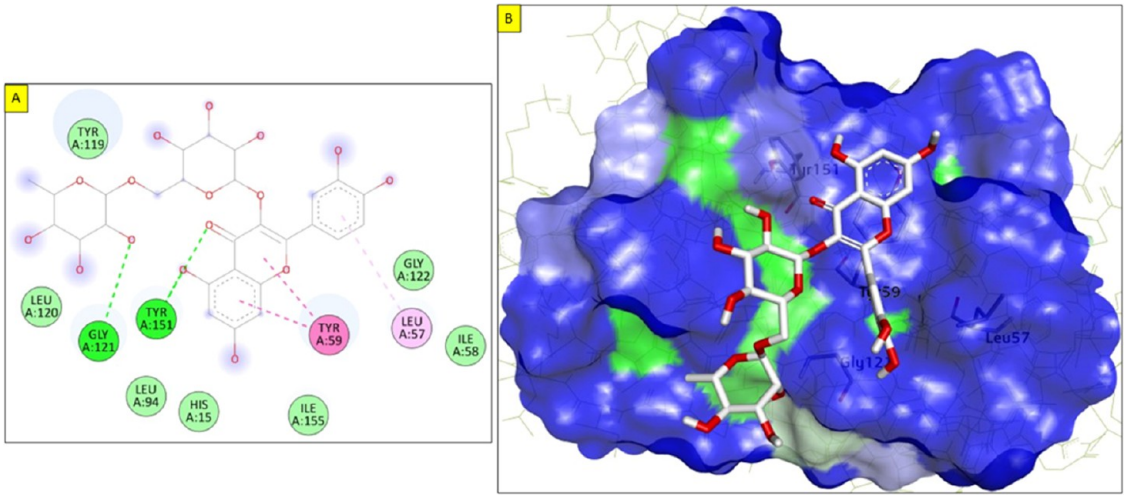

Figure 9. Molecular docking of rutin with TNF-α: (A) 2D interaction of rutin with TNF-α, and (B) surface view of the best-docked pose in the binding site of the protein.

4. DISCUSSION

The escalating global prevalence of diabetes has raised significant public and scientific concerns due to its profound impact on patients' health, quality of life, and medical expenditures. One of the major complications associated with uncontrolled hyperglycemia is impaired wound healing, which, if left untreated, can lead to severe outcomes, such as gangrene and amputation.[36] It is estimated that 75% of the one million annual leg amputations worldwide are due to type 2 diabetes, underscoring the urgent need for effective interventions to address this critical health issue. Recently, bioactive compounds have garnered significant interest as potential agents for managing wound healing in hyperglycemic individuals. Among such compounds, rutin is well known for its various pharmacological effects. Therefore, this study aimed to explore the potential protective role of the topical application of rutin-NPs in wound healing in STZ-induced diabetic rats treated with metformin.

The current research involved inducing diabetes in rats using STZ. Diabetic rats showed a significant increase in blood glucose levels after 72 h, which persisted throughout the experimental period. These findings align with those of previous studies.[37,38] Additionally, treating diabetic rats with metformin and the topical application of rutin-NPs resulted in a significant reduction in their blood glucose levels. Additionally, patients with type 2 diabetes often exhibit dyslipidemia and metabolic changes in their triglyceride-rich lipoproteins.[39] In this study, diabetic wound rats displayed a significant increase in total cholesterol, triglycerides, and LDL cholesterol levels and a significant decrease in HDL cholesterol levels. However, treating diabetic wounds with metformin and topical application of rutin-NPs coordinated effectively and significantly reduced total cholesterol, triglyceride, and LDL cholesterol levels and led to a significant increase in HDL cholesterol levels.

ROS plays a beneficial role in combating microbial invasion and regulating intracellular signaling pathways under normal physiological conditions. However, in diabetic patients, elevated blood glucose levels lead to oxidative stress, which disrupts the wound-healing process by causing uncontrolled inflammation.[40] Excessive oxidative stress can harm proteins, lipids, and DNA within cells, eventually leading to cell death and subsequent tissue malfunction.[41] Clinical research has demonstrated that

https://doi.org/10.1021/acsomega.3c05595
ACS Omega 2024, 9, 32394−32406

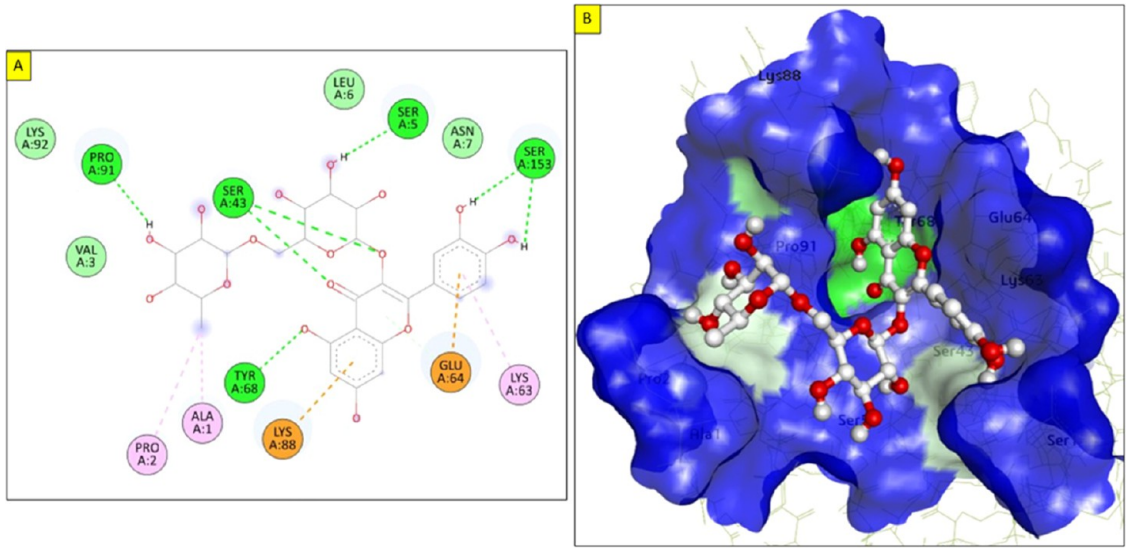

Figure 10. Molecular docking of rutin with IL-1β: (A) 2D interaction of rutin with IL-6, and (B) surface view of the best-docked pose in the binding site of the protein.

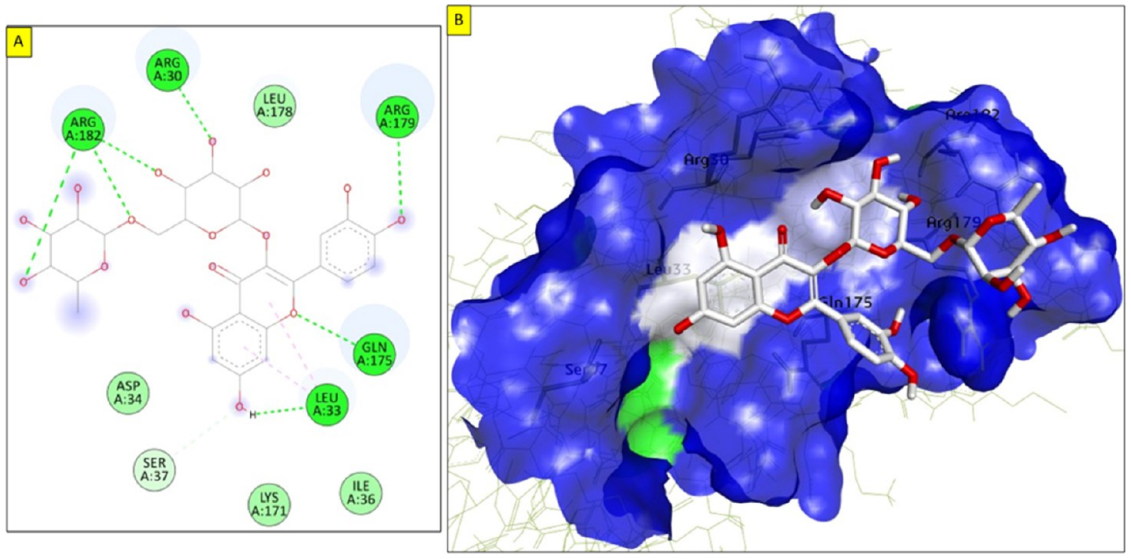

Figure 11. Molecular docking of rutin with IL-6: (A) 2D interaction of rutin with IL-6, and (B) surface view of the best-docked pose in the binding site of the protein.

wound tissues in diabetic patients experience more severe oxidative stress than wound skin tissues in nondiabetic patients.[42] Nrf2 is an integral component of the cellular defense system and is activated in response to high levels of oxidative stress. When the cells are exposed to oxidative stress, Nrf2 dissociates from its cytoplasmic inhibitor, Keap-1, and translocates into the nucleus to promote the transcription of many cytoprotective genes.[43] Nrf2 has emerged as a promising therapeutic target for treating diabetic and nondiabetic wounds.[44] Nrf2 activation can reduce oxidative stress and expedite wound healing in diabetic mice.[42] In line with prior research, our study found that diabetic control rats had reduced levels of the skin antioxidants GSH, CAT, and SOD, as well as increased MDA production. These results are consistent with earlier findings.[45,46] Nevertheless, topical rutin-NPs alleviated these effects, boosted antioxidant levels, and reduced MDA production. Furthermore, we observed that diabetic control rats with wounds exhibited upregulation of Keap-1 levels and reduced Nrf2 expression levels compared with the control group. Notably, the application of rutin-NPs reversed this effect, increased Keap-1 expression, and upregulated Nrf2 expression.

Numerous proinflammatory cytokines delay the healing process as these cytokines and proteinases destroy the tissue and develop chronic wounds. Previous studies have shown that impaired wound healing in diabetic rats is linked to a significant upregulation of proinflammatory cytokines, such as IL-1β, IL-6, and TNF-α.[47] In agreement with this, our data revealed that STZ-wounded rats experienced higher levels of CRP and proinflammatory cytokines TNF-α, IL-1β, and IL-6. Intriguingly, the application of rutin-NPs attenuated this increment significantly. These data are aligned with several previous studies that concluded the anti-inflammatory effects of rutin in different experimental models.[48−51]

Molecular docking confirmed the biological results of rutin, which was docked into the catalytic site of the X-ray crystallographic structures of CRP, Keap-1, IL-1β, IL-6, and

https://doi.org/10.1021/acsomega.3c05595
ACS Omega 2024, 9, 32394−32406

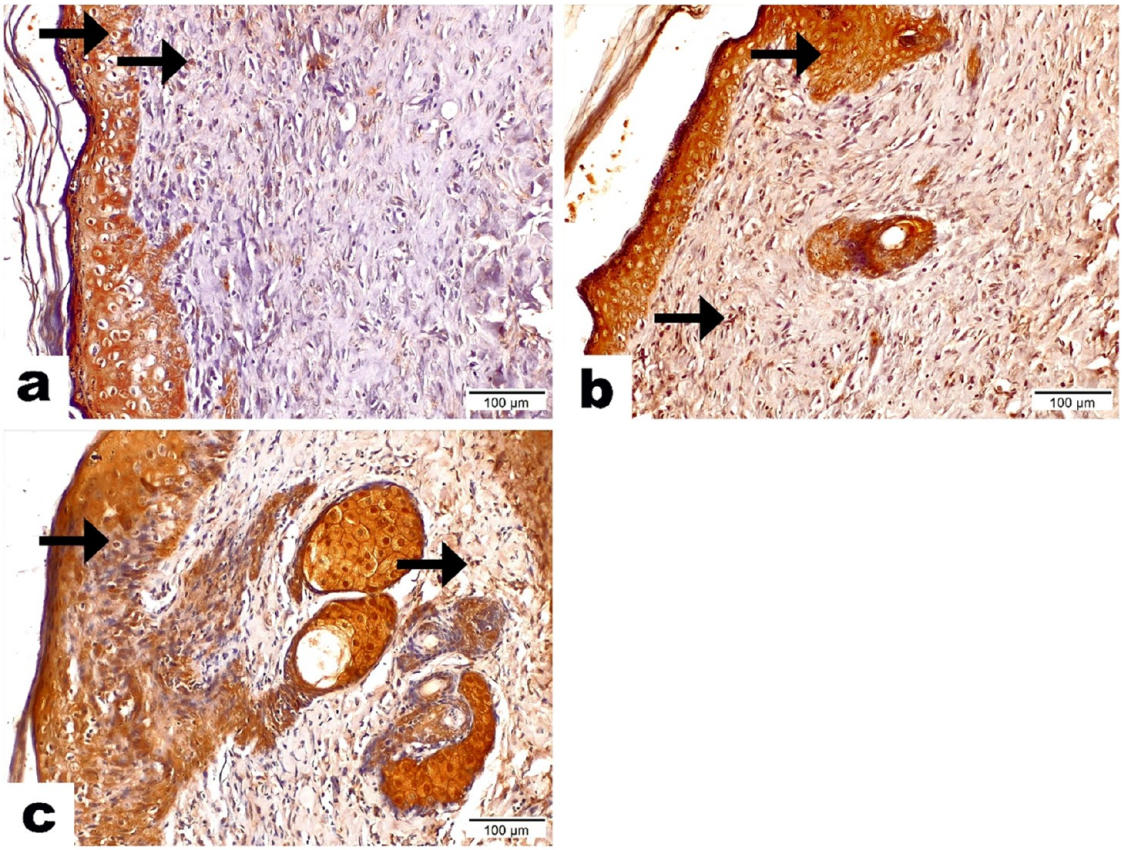

Figure 12. Topical preparation of rutin-NPs upregulated K_i-67 in STZ-induced diabetic rats. Photomicrographs represented the immunoreactivity of K_i-67 antibody in skin tissues at 21 days between the tested groups (K_i-67 antibody, magnification power = ×200, scale bar = 100 μm). (a) The skin section from the untreated control group displayed low expression of K_i-67 antibody (+) with cytoplasmic and nuclear reactivity all along the epidermis and dermis layers (arrows). (b) The skin section from the rutin-NP-treated group showed moderate expression of the K_i-67 antibody (++) with cytoplasmic and nuclear reactivity of the epidermis and dermis layers (arrows) with a significant difference from the negative control group. (c) The skin section from the β-sitosterol(standard) group showed the highest expression of K_i-67 antibody (+++) with cytoplasmic and nuclear reactivity of the epidermis and dermis layers (arrows) with a significant difference from the untreated control group and rutin-NP group.

TNF-α via grid-based ligand docking. The binding affinity and the binding energy of ligand−protein interactions demonstrated the affinity and binding to the specifically selected proteins.

Finally, the skin section from the rutin-NP-treated group showed moderate expression of K_i-67 antibody with cytoplasmic and nuclear reactivity of the epidermis and dermis layers with a significant difference from the negative control group and a significant difference from the untreated control group and rutin-NP group. Skin sections from the rutin-NP application group showed the regenerated collagen bundles with the regular arrangement and extensive distribution homing the dermal layer. These data demonstrated the promotion of cell proliferation at the wound site and significantly accelerated wound closure, which was accompanied by the facilitated regeneration of granulation tissue.

5. CONCLUSIONS

These findings suggest that rutin-NPs have the potential to enhance the wound-healing process by attenuating oxidative stress and inflammation through their modulatory effects on the Keap-1/Nrf2 pathway. Moreover, these results underscore the therapeutic potential of rutin-NPs as a natural wound-healing agent. Molecular docking was used to confirm the biological effects of rutin. Further studies are needed to elucidate the mechanisms underlying rutin's beneficial effects on wound healing and its potential clinical application.

AUTHOR INFORMATION

Corresponding Author

Steve Harakeh − *King Fahd Medical Research Center, Faculty of Medicine, King Abdulaziz University, Jeddah 21589, Saudi Arabia; Yousef Abdul Latif Jameel Scientific Chair of Prophetic Medicine Application, Faculty of Medicine, KAU, Jeddah 21589, Saudi Arabia;* orcid.org/0000-0001-7512-8787; Email: sharakeh@gmail.com

Authors

Manal Naseeb − *Department of Clinical Nutrition, Faculty of Applied Medical Sciences, King Abdulaziz University, Jeddah 21589, Saudi Arabia;* orcid.org/0000-0002-6851-5276

Eram Albajri − *Department of Clinical Nutrition, Faculty of Applied Medical Sciences, King Abdulaziz University, Jeddah 21589, Saudi Arabia*

Arwa Almasaudi − *Department of Clinical Nutrition, Faculty of Applied Medical Sciences, King Abdulaziz University, Jeddah 21589, Saudi Arabia*

Turki Alamri − *Family and Community Medicine Department, Faculty of Medicine in Rabigh, King Abdulaziz University, Jeddah 21589, Saudi Arabia;* orcid.org/0000-0003-4382-4109

https://doi.org/10.1021/acsomega.3c05595
ACS Omega 2024, 9, 32394−32406

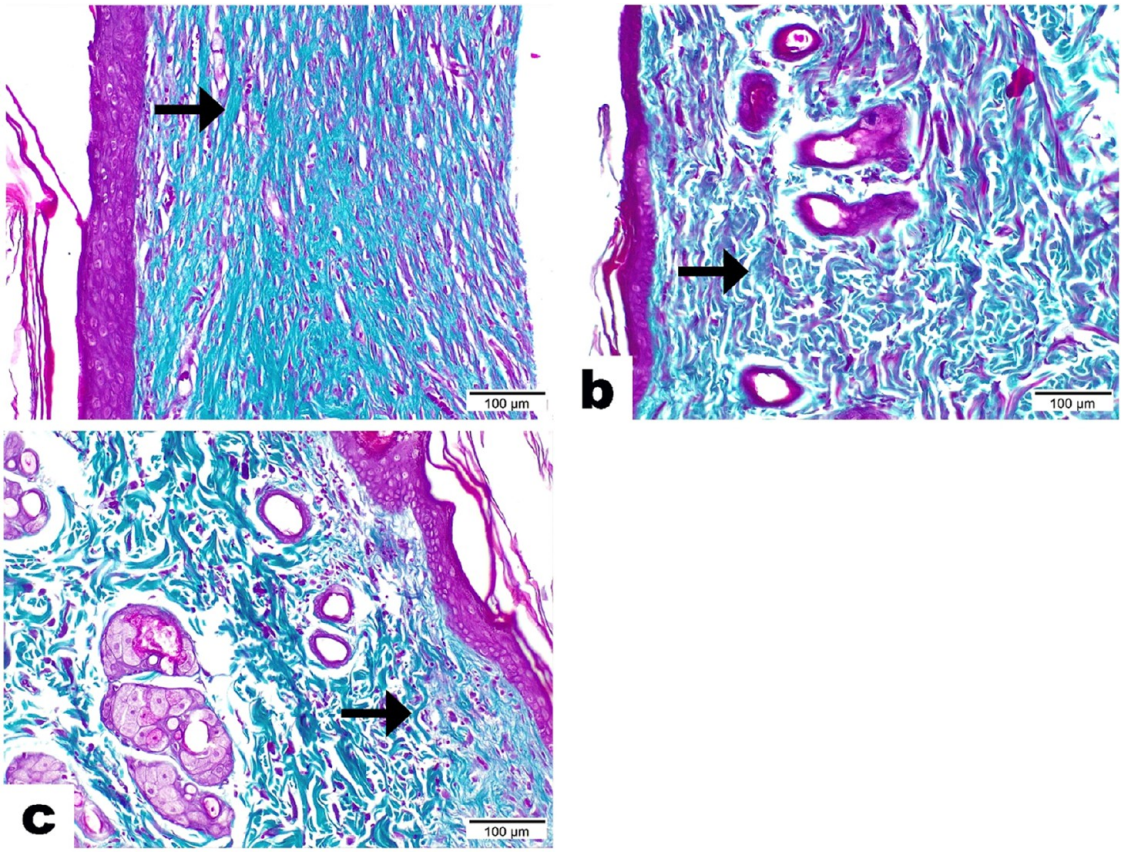

Figure 13. Effect of topical preparation of rutin-NPs on skin fibrosis of skin stained with Masson's trichrome stain in STZ-induced diabetic rats. Photomicrographs demonstrated the proliferation of green collagen fibers in skin tissues at 21 days between the tested groups stained with Masson's trichrome stain (magnification power = ×200, scale bar = 100 μm). (a) The skin section from the untreated control group showed a loosely packed and irregular arrangement of collagen fibers along the dermis layer (arrow). (b) Skin sections from the application of rutin-NP and the β-sitosterol (standard) group showed the regenerated collagen bundles with regular arrangement and extensive distribution homing the dermal layer (arrow).

Hatoon A. Niyazi − *Department of Clinical Microbiology and Immunology, Faculty of Medicine, King Abdulaziz University, Jeddah 21589, Saudi Arabia*

Soad Aljaouni − *Department of Haematology/Pediatric Oncology, KAUH, Faculty of Medicine (FM) and Yousef Abdul Latif Jameel Scientific Chair of Prophetic Medicine Application, Faculty of Medicine, KAU, Jeddah 21589, Saudi Arabia*

Abdulrahman B. O. Mohamed − *Department of Pharmacology, Faculty of Medicine, King Abdulaziz University (KAU), Jeddah 21589, Saudi Arabia (SA)*

Hanouf A. Niyazi − *Department of Clinical Microbiology and Immunology, Faculty of Medicine, King Abdulaziz University, Jeddah 21589, Saudi Arabia*

Ahmed S. Ali − *Department of Pharmacology, Faculty of Medicine, King Abdulaziz University (KAU), Jeddah 21589, Saudi Arabia (SA)*

Soad Shaker Ali − *Department of Anatomy, Faculty of Medicine, King Abdulaziz University, Jeddah 21589, Saudi Arabia*

Saber H. Saber − *Laboratory of Molecular Cell Biology, Department of Zoology, Faculty of Science, Assiut University, Assiut 2063045, Egypt*

Huda Ahmed Abuaraki − *Animal Unit, King Fahd Medical Research Center, Faculty of Medicine, King Abdulaziz University, Jeddah 21589, Saudi Arabia*

Shafiul Haque − *Research and Scientific Studies Unit, College of Nursing and Health Sciences, Jazan University, Jazan 45142, Saudi Arabia; Gilbert and Rose-Marie Chagoury School of Medicine, Lebanese American University, Beirut 11022801, Lebanon; Centre of Medical and Bio-Allied Health Sciences Research, Ajman University, Ajman 13306, United Arab Emirates;* orcid.org/0000-0002-2989-121X

Complete contact information is available at: https://pubs.acs.org/10.1021/acsomega.3c05595

Notes

The authors declare no competing financial interest.

■ ACKNOWLEDGMENTS

The Deanship of Scientific Research (DSR) at King Abdulaziz University (KAU), Jeddah, Saudi Arabia has funded this project under grant number G: 665-290-1443. The authors express their gratitude to the DSR for their technical and financial assistance.

■ REFERENCES

(1) Ogurtsova, K.; da Rocha Fernandes, J.; Huang, Y.; Linnenkamp, U.; Guariguata, L.; Cho, N. H.; Cavan, D.; Shaw, J.; Makaroff, L.J.D.r.; practice, c. IDF Diabetes Atlas: Global estimates for the prevalence of diabetes for 2015 and 2040. *Diabetes Res. Clin. Pract.* **2017**, *128*, 40−50.

(2) Ali, R.; Khamis, T.; Enan, G.; El-Didamony, G.; Sitohy, B.; Abdel-Fattah, G. The Healing Capability of Clove Flower Extract (CFE) in Streptozotocin-Induced (STZ-Induced) Diabetic Rat Wounds Infected

with Multidrug Resistant Bacteria. *Molecules* **2022**, *27* (7), No. 2270, DOI: 10.3390/molecules27072270.
(3) Li, Q.; Liang, S.; Lai, Q.; Shen, L.; Zhang, Y.; Guo, R. Heme oxygenase-1 alleviates advanced glycation end product-induced oxidative stress, inflammatory response and biological behavioral disorders in rat dermal fibroblasts. *Exp. Ther. Med.* **2021**, *22* (5), No. 1212.
(4) Teng, M.; Li, Z.; Wu, X.; Zhang, Z.; Lu, Z.; Wu, K.; Guo, J. Development of tannin-bridged cerium oxide microcubes-chitosan cryogel as a multifunctional wound dressing. *Colloids Surf., B* **2022**, *214*, No. 112479.
(5) Matsubara, Y.; Kumamoto, H.; Iizuka, Y.; Murakami, T.; Okamoto, K.; Miyake, H.; Yokoi, K. Structure and hypotensive effect of flavonoid glycosides in Citrus unshiu peelings. *Agric. Biol. Chem.* **1985**, *49* (4), 909−914.
(6) Kreft, S.; Knapp, M.; Kreft, I. Extraction of rutin from buckwheat (Fagopyru esculentumMoench) seeds and determination by capillary electrophoresis. *J. Agric. Food Chem.* **1999**, *47* (11), 4649−4652.
(7) Nafees, S.; Rashid, S.; Ali, N.; Hasan, S. K.; Sultana, S. Rutin ameliorates cyclophosphamide induced oxidative stress and inflammation in Wistar rats: role of NFκB/MAPK pathway. *Chem. Biol. Interact.* **2015**, *231*, 98−107.
(8) Ganeshpurkar, A.; Saluja, A. K. The Pharmacological Potential of Rutin. *Saudi Pharm. J.* **2017**, *25* (2), 149−164.
(9) Aruna, R.; Geetha, A.; Suguna, P.; Suganya, V. Rutin rich Emblica officinalis Geart. fruit extract ameliorates inflammation in the pancreas of rats subjected to alcohol and cerulein administration. *J. Complementary Integr. Med.* **2014**, *11* (1), 9−18.
(10) Song, K.; Na, J. Y.; Kim, S.; Kwon, J. Rutin upregulates neurotrophic factors resulting in attenuation of ethanol-induced oxidative stress in HT22 hippocampal neuronal cells. *J. Sci. Food Agric.* **2015**, *95* (10), 2117−2123.
(11) Anlas, C.; Bakirel, T.; Ustun-Alkan, F.; Celik, B.; Baran, M. Y.; Ustuner, O.; Kuruuzum-Uz, A. In vitro evaluation of the therapeutic potential of Anatolian kermes oak (Quercus coccifera L.) as an alternative wound healing agent. *Ind. Crops Prod.* **2019**, *137*, 24−32.
(12) Davis, S. C.; Perez, R. Cosmeceuticals and natural products: wound healing. *Clin. Dermatol.* **2009**, *27* (5), 502−506.
(13) Ibrahim, N.; Wong, S. K.; Mohamed, I. N.; Mohamed, N.; Chin, K. Y.; Ima-Nirwana, S.; Shuid, A. N. Wound Healing Properties of Selected Natural Products. *Int. J. Environ. Res. Public Health* **2018**, *15* (11), No. 2360, DOI: 10.3390/ijerph15112360.
(14) Tsala, D. E.; Amadou, D.; Habtemariam, S. Natural wound healing and bioactive natural products. *Phytopharmacology* **2013**, *4* (3), 532−560.
(15) Naskar, A.; Kim, K. S. Recent Advances in Nanomaterial-Based Wound-Healing Therapeutics. *Pharmaceutics* **2020**, *12* (6), No. 499, DOI: 10.3390/pharmaceutics12060499.
(16) Watkins, R.; Wu, L.; Zhang, C.; Davis, R. M.; Xu, B. Natural product-based nanomedicine: recent advances and issues. *Int. J. Nanomed.* **2015**, *10*, 6055−6074.
(17) Alam, S.; Khan, Z. I.; Mustafa, G.; Kumar, M.; Islam, F.; Bhatnagar, A.; Ahmad, F. J. Development and evaluation of thymoquinone-encapsulated chitosan nanoparticles for nose-to-brain targeting:a pharmacoscintigraphic study. *Int. J. Nanomed.* **2012**, *7*, 5705−5718.
(18) Almuhayawi, M. S.; Ramadan, W. S.; Harakeh, S.; Al Jaouni, S. K.; Bharali, D. J.; Mousa, S. A.; Almuhayawi, S. M. The potential role of pomegranate and its nano-formulations on cerebral neurons in aluminum chloride induced Alzheimer rat model. *Saudi J. Biol. Sci.* **2020**, *27* (7), 1710−1716.
(19) El-Shitany, N.A.E.-A.; Abbas, A. T.; Ali, S. S.; Eid, B.; Harakeh, S.; Neamatallah, T.; Al-Abd, A.; Mousa, S. Nanoparticles Ellagic Acid Protects Against Cisplatin-induced Hepatotoxicity in Rats Without Inhibiting its Cytotoxic Activity. *Int. J. Pharmacol.* **2019**, *15* (4), 465−477.
(20) Cannon, C. Z.; Kissling, G. E.; Goulding, D. R.; King-Herbert, A. P.; Blankenship-Paris, T. Analgesic effects of tramadol, carprofen or multimodal analgesia in rats undergoing ventral laparotomy. *Lab. Anim.* **2011**, *40* (3), 85−93.
(21) Abbasnezhad, A.; Niazmand, S.; Mahmoudabady, M.; Soukhtanloo, M.; Rezaee, S. A.; Mousavi, S. M. Nigella sativa seed decreases endothelial dysfunction in streptozotocin-induced diabetic rat aorta. *Avicenna J. Phytomed.* **2016**, *6* (1), 67−76.
(22) Bancroft, J. D.; Stevens, A. *Theory and Practice of Histological Techniques*, 7th ed.; Churchill Livingstone: London, 2013; pp 120−131.
(23) Ellman, G. L. Tissue sulfhydryl groups. *Arch. Biochem. Biophys.* **1959**, *82* (1), 70−77.
(24) Mihara, M.; Uchiyama, M. Determination of malonaldehyde precursor in tissues by thiobarbituric acid test. *Anal. Biochem.* **1978**, *86* (1), 271−278.
(25) Aebi, H. Catalase in Vitro. In *Methods in Enzymology*; Academic Press, 1984; pp 121−126.
(26) Marklund, S. L. Superoxide dismutase isoenzymes in tissues and plasma from New Zealand black mice, nude mice and normal BALB/c mice. *Mutat. Res., Fundam. Mol. Mech. Mutagen.* **1985**, *148* (1−2), 129−134.
(27) Van Weemen, B.; Schuurs, A. Immunoassay using antigen—enzyme conjugates. *FEBS Lett.* **1971**, *15* (3), 232−236.
(28) Thompson, D.; Pepys, M. B.; Wood, S. P. The physiological structure of human C-reactive protein and its complex with phosphocholine. *Structure* **1999**, *7* (2), 169−177.
(29) Jnoff, E.; Albrecht, C.; Barker, J. J.; Barker, O.; Beaumont, E.; Bromidge, S.; Brookfield, F.; Brooks, M.; Bubert, C.; Ceska, T.; Corden, V.; Dawson, G.; Duclos, S.; Fryatt, T.; Genicot, C.; Jigorel, E.; Kwong, J.; Maghames, R.; Mushi, I.; Pike, R.; Sands, Z. A.; Smith, M. A.; Stimson, C. C.; Courade, J.-P. Binding Mode and Structure−Activity Relationships around Direct Inhibitors of the Nrf2−Keap1Complex. *ChemMedChem* **2014**, *9* (4), 699−705.
(30) Yu, B.; Blaber, M.; Gronenborn, A. M.; Clore, G. M.; Caspar, D. L. D. Disordered water within a hydrophobic protein cavity visualized by x-ray crystallography. *Proc. Natl. Acad. Sci. U.S.A.* **1999**, *96* (1), 103−108.
(31) Somers, W.; Stahl, M.; Seehra, J. S. 1.9 Å crystal structure of interleukin 6: implications for a novel mode of receptor dimerization and signaling. *EMBO J.* **1997**, *16* (5), 989−997.
(32) He, M. M.; Smith, A. S.; Oslob, J. D.; Flanagan, W. M.; Braisted, A. C.; Whitty, A.; Cancilla, M. T.; Wang, J.; Lugovskoy, A. A.; Yoburn, J. C.; Fung, A. D.; Farrington, G.; Eldredge, J. K.; Day, E. S.; Cruz, L. A.; Cachero, T. G.; Miller, S. K.; Friedman, J. E.; Choong, I. C.; Cunningham, B. C. Small-Molecule Inhibition of TNF-alpha. *Science* **2005**, *310* (5750), 1022−1025.
(33) O'Boyle, N. M.; Banck, M.; James, C. A.; Morley, C.; Vandermeersch, T.; Hutchison, G. R. Open Babel: An open chemical toolbox. *J. Cheminf.* **2011**, *3* (1), No. 33.
(34) Trott, O.; Olson, A. J. AutoDock Vina: Improving the speed and accuracy of docking with a new scoring function, efficient optimization, and multithreading. *J. Comput. Chem.* **2010**, *31* (2), 455−461.
(35) Biovia, D. S. J. S. D., Discovery Studio Visualizer, CA, USA, *936* (2017).
(36) Rossing, P. Diabetic nephropathy: worldwide epidemic and effects of current treatment on natural history. *Curr. Diab. Rep.* **2006**, *6* (6), 479−483.
(37) Pauzi, N. A. S.; Muhammad, A.; Fakurazi, S.; Arulselvan, P.; Ahmad, Z. Preliminary study of the optimization of protocol for development of type 2 diabetic model in rats. *Indian J. Sci. Technol.* **2013**, *6* (7), 4960−4965.
(38) Pimple, B. P.; Kadam, P.; Patil, M. J. Comparative antihyperglycaemic and antihyperlipidemic effect of Origanum majorana extracts in NIDDM rats. *Orient. Pharm. Exp. Med.* **2012**, *12* (1), 41−50.
(39) Gylling, H.; Hallikainen, M.; Pihlajamäki, J.; Ågren, J.; Laakso, M.; Rajaratnam, R. A.; Rauramaa, R.; Miettinen, T. Polymorphisms in the ABCG5 and ABCG8 genes associate with cholesterol absorption and insulin sensitivity. *J. Lipid Res.* **2004**, *45* (9), 1660−1665.
(40) Jindam, A.; Yerra, V. G.; Kumar, A. Nrf2: a promising trove for diabetic wound healing. *Ann. Transl Med.* **2017**, *5* (23), 469.

https://doi.org/10.1021/acsomega.3c05595
ACS Omega 2024, 9, 32394−32406

(41) Tabak, O.; Gelisgen, R.; Erman, H.; Erdenen, F.; Muderrisoglu, C.; Aral, H.; Uzun, H. J. C.; Medicine, I. Oxidative lipid, protein, and DNA damage as oxidative stress markers in vascular complications of diabetes mellitus. *Clin. Invest. Med.* **2011**, *34*, E163−E171.
(42) Long, M.; Rojo de la Vega, M.; Wen, Q.; Bharara, M.; Jiang, T.; Zhang, R.; Zhou, S.; Wong, P. K.; Wondrak, G. T.; Zheng, H. J. D.; Zhang, D. D. An essential role of NRF2 in diabetic wound healing. *Diabetes* **2016**, *65* (3), 780−793.
(43) Chang, A. S.; Hathaway, C. K.; Smithies, O.; Kakoki, M. Transforming growth factor-β1and diabetic nephropathy. *Am. J. Physiol. Renal. Physiol.* **2016**, *310* (8), F689−F696.
(44) Hayashi, R.; Himori, N.; Taguchi, K.; Ishikawa, Y.; Uesugi, K.; Ito, M.; Duncan, T.; Tsujikawa, M.; Nakazawa, T.; Yamamoto, M. J. F. R. B. Medicine, The role of the Nrf2-mediated defense system in corneal epithelial wound healing. *Free Radical Biol. Med.* **2013**, *61*, 333−342.
(45) Giacco, F.; Brownlee, M.J.C.r. Oxidative stress and diabetic complications. *Circ. Res.* **2010**, *107* (9), 1058−1070.
(46) Matough, F. A.; Budin, S. B.; Hamid, Z. A.; Alwahaibi, N.; Mohamed, J. The role of oxidative stress and antioxidants in diabetic complications. *Sultan Qaboos Univ. Med. J.* **2012**, *12* (1), 5.
(47) Ponrasu, T.; Suguna, L. Efficacy of Annona squamosa on wound healing in streptozotocininduced diabetic rats. *Int. Wound J.* **2012**, *9* (6), 613−623.
(48) Muvhulawa, N.; Dludla, P. V.; Ziqubu, K.; Mthembu, S. X. H.; Mthiyane, F.; Nkambule, B. B.; Mazibuko-Mbeje, S. E. Rutin ameliorates inflammation and improves metabolic function: A comprehensive analysis of scientific literature. *Pharmacol. Res.* **2022**, *178*, No. 106163.
(49) Li, B.; Ji, Y.; Yi, C.; Wang, X.; Liu, C.; Wang, C.; Lu, X.; Xu, X.; Wang, X. Rutin Inhibits Ox-LDL-Mediated Macrophage Inflammation and Foam Cell Formation by Inducing Autophagy and Modulating PI3K/ATK Signaling. *Molecules* **2022**, *27* (13), No. 4201, DOI: 10.3390/molecules27134201.
(50) Amjadi, S.; Shahnaz, F.; Shokouhi, B.; Azarmi, Y.; Siahi-Shadbad, M.; Ghanbarzadeh, S.; Kouhsoltani, M.; Ebrahimi, A.; Hamishehkar, H. Nanophytosomes for enhancement of rutin efficacy in oral administration for diabetes treatment in streptozotocin-induced diabetic rats. *Int. J. Pharm.* **2021**, *610*, No. 121208.
(51) Wang, Y. B.; Ge, Z. M.; Kang, W. Q.; Lian, Z. X.; Yao, J.; Zhou, C. Y. Rutin alleviates diabetic cardiomyopathy in a rat model of type 2 diabetes. *Exp. Ther. Med.* **2015**, *9* (2), 451−455.

https://doi.org/10.1021/acsomega.3c05595
ACS Omega 2024, 9, 32394−32406